SIMULATION OF ELECTRICAL POWER SYSTEMS OF GREECE (CRETE) USING THE InterPSS

Dionysia Svarna[1],
[0009-0005-1673-6084]

Alexios Serafeim Nterekas[2]*,
[0009-0006-4806-4574]

Georgia Ntereka[3]
[0009-0008-6108-3387]

[1]Medical University of Sofia,
Faculty of Pharmacy,
Sofia, Bulgaria

[2]Technical University of Crete,
Management Systems Laboratory,
School of Production Engineering and Management,
Chania, Greece

Correspondence:
Alexios Serafeim Nterekas

e-mail:
anterekas@tuc.gr

Abstract:

The electrical power system network is a highly complex and extensive entity, particularly when incorporating distributed generation, renewable energy sources, and energy storage devices. This research examines the load flow analysis of the Crete electrical grid using the Internet Technology based Power System Simulator (InterPSS). The Crete electrical network, consisting of 16 buses, was simulated under two scenarios. In the first scenario, the loads absorb 81.5% of their maximum power and 100% of the wind generation. In the second scenario, the loads remain the same, but the wind generation is multiplied by a factor of 5.4, resulting in a total of 1000MW=10 P.U.

The results show that in the first scenario, the voltages remain within permissible limits, and no power flow overloading occurs in the network branches, ensuring that the system operates without issues. However, in the second scenario, although the voltage remains within permissible limits, overloading is observed in several branches, making it possible for the system to operate under these conditions.

Keywords:

Simulation, Electrical Power System Network, Renewable Energy Sources, Load Flow Analysis, Internet Technology based Power System Simulator.

INTRODUCTION

The integration of renewable energy technologies and strategies for improving energy efficiency has become increasingly crucial to meet the ambitious target of reducing greenhouse gas emissions by 2050 [1]. To achieve a sustainable balance between energy production and consumption, several changes must still be addressed. These challenges are closely tied to the rising demand for energy [2], driven by industrial and economic growth in both developed and emerging nations [3]. Consequently, many countries have recognized the need to create and implement a new, sustainable energy framework across key sectors, including buildings, transportation, and industry. This new framework must be diverse and adaptable, incorporating principles such as the waste-to-energy approach [4], energy consumption reduction, the circular economy [5], improved quality of life for people [6], pollution mitigation and climate change adaptation [7], and the overarching goal of achieving carbon neutrality and zero emissions by 2050 [8].

CC BY

DOI: 10.15308/Sinteza-2025-184-192

Furthermore, to enhance the adoption of renewable energy in society, it is essential to carefully address issues related to the management of surplus renewable electricity generation [9]. This surplus can lead to significant challenges in terms of grid stability and management [10].

The primary objective of this research is to examine the load flow analysis of the Crete electrical grid using the Internet Technology based Power System Simulator (InterPSS). InterPSS has been used widely in research to design, analysis, and simulation of power systems [11].

2. INTERNET TECHNOLOGY BASED POWER SYSTEM SIMULATOR (INTERPSS)

The InterPSS (Internet technology based Power System Simulator) is a free and open-source software tool for the design, analysis, diagnosis, and operation of electrical power systems. It provides a flexible and extensible platform that allows researchers and developers to expand the simulation engine or adapt the platform for domain-specific or cross-domain power system simulation applications [11], [12]. InterPSS is both easy to use and highly functional. While many existing power system simulation tools rely on outdated technologies, InterPSS distinguishes itself through its open and loosely coupled architecture. This innovative design enables components developed by other users to be easily integrated into the InterPSS environment, enhancing its functionality. At the same time, InterPSS components can be effortlessly incorporated into other software systems [11], [12]. The present research examines the load flow analysis of the Cretan power grid under two scenarios. The second scenario is simulated in the same manner as the first, with the only difference being that the wind power generation is multiplied by a factor of 5.4, resulting in a total of 1000 MW = 10 P.U. The software includes a graphical editor that allows users to create one-line diagrams and input the necessary data [11], [12]. The latest version offers essential features such as creating simple one-line diagrams of power systems, entering data, executing simulations, and generating reports. The electrical grid of Crete, consisting of 16 buses, is described below, with its topology illustrated in Figure 1 [13] (buses: 1-Chania, 2-Heraklion, 3-Atherinolakkou, 4-Sitia, 5-Agios Nikolaos, 6-Ierapetra, 7-Stalida, 8-Praitorion, 9-Moires, 10-Agias Barbaras, 11-Ammou, 12-Spili, 13-Rethumno, 14-Vrisses, 15-Aguias, 16-Kissamos). The design of the Cretan grid in InterPSS is depicted in Figure 2.

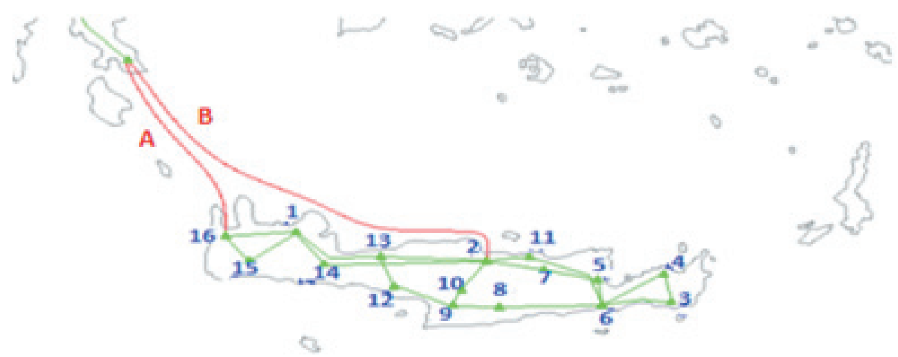

Figure 1. Buses [13]

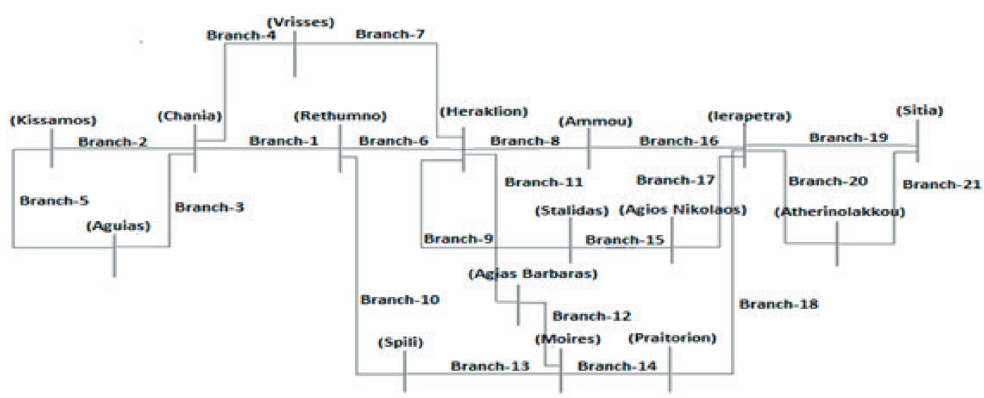

Figure 2. Electricity network of Crete in the InterPSS

3. RESEARCH METHOD

3.1. DATA ENTRY IN THE INTERPSS

The classification of buses (PV, PQ, and Swing) and the calculations of load and branch data are presented in Tables 1, and 2. Branch Data: To complete the dataset for each branch, their lengths were estimated approximately using Google Maps [11]. The data used to calculate the complex impedance of each branch are as follows: For branch type E/150: R(P.U.)= 0,000812, X(P.U.)= 0,001795, B(P.U.)= 0,00197. For branch type B/150: R(P.U.)= 0,000433, X(P.U.)= 0,001875, B(P.U.)= 0,001924. The power transmission limits applied for the 150 kV transmission lines are: MVARating1= 202 MVA, MVARating2= 124 MVA, MVARating3= 170 MVA [14]. Bus data: The calculations for each bus category are outlined below. Buses PV: Pgen (P.U.) is determined by summing all power outputs from conventional generation units connected to the same bus. The total generation is then divided by 100 MVA, which serves as the base power value [15]. Vspec (P.U.)= 1,02 for all PV and Swing buses [14]. Pload (P.U.) is divided by 100 MVA, which is the base price for power [16]. Qload (P.U.) is calculated by the type $Q_{load} = P_{load} \cdot (\sqrt{1-0.85^2} / 0.85)$ where 0.85 is the power factor (cosφ) of the load. Buses PQ: Pgen (P.U.)= +Pwind, where Pwind is from wind power production. The total production will be divided by 100 MVA which is the base price for power. Qgen (P.U.)= Qw [17], is calculated by the type $Q_w = -P_{wind} \cdot (\sqrt{1-0.85^2} / 0.85)$. Qload (P.U.) is calculated by the type $Q_{load} = P_{load} \cdot (\sqrt{1-0.85^2} / 0.85)$ where 0.85 is the power factor (cosφ) of the load [18].

In the second scenario, the simulation was conducted in the same manner as Scenario 1, with the key difference being that wind generation was multiplied by a factor of 5.4, resulting in a total power output of 1000 MW = 10 P.U. The data used in this scenario are presented below. The calculations performed for each bus are presented in Table 2.

3.2. FACE VALIDITY AND MEASURES

The face validity of the research was carefully assessed through the selection of realistic scenarios, ensuring that the results of the power flow study reflect what would be expected in a real-world power system. The scenarios chosen were based on expert input and industry standards, ensuring that the conditions modeled in the InterPSS software accurately represent typical operational states of modern power grids [14], [15].

Table 1. Calculations for each bus - First Scenario

Buses	Type	cosφ	Pgen (P.U.)	Vspec (P.U.)	Qgen (P.U.)	Pload (P.U.)	Qload (P.U.)
Chania	PV	0.85	2	1.02		1.26325	0.805228488
Heraklion	PV	0.85	1.98	1.02		0.9291	0.596110331
Atherinolakkou	PV	0.85	1.01	1.02		0.1467	0.090916494
Sitia	PQ	0.85	0.89		0.1807222	0.163	0.101018327
Agios Nikolaos	PQ	0.85	0.12		-0.024367	0.4564	0.282851316
Ierapetra	PQ	0.85	0		0	0.20375	0.126272909
Stalida	PQ	0.85	0		0	0.6357	0.393971476
Praitorion	PQ	0.85	0		0	0.13855	0.085865578
Moires	PQ	0.85	0.18		0.0365506	0.38305	0.237393069
Agias Barbaras	PQ	0.85	0.15		0.0304588	0.12225	0.075763745
Ammou	PQ	0.85	0		0	0.7498	0.464684305
Spili	PQ	0.85	0		0	0.1956	0.121221993
Rethumno	PQ	0.85	0.1		0.0203059	0.6846	0.424276974
Vrisses	PQ	0.85	0		0	0.2282	0.141425658
Aguias	PQ	0.85	0		0	0.1304	0.080814662
Kissamos	Swing	0.85	0.19	1.02	-0.0385811	0.163	0.101018327

Table 2. Calculations for each bus - Second scenario

Buses	Type	cosφ	Pgen (P.U.)	Vspec (P.U.)	Qgen (P.U.)	Pload (P.U.)	Qload (P.U.)
Chania	PV	0.85	2.4873	1.02		1.26325	0.912443461
Heraklion	PV	0.85	2.423	1.02		0.9291	0.695202957
Atherinolakkou	PV	0.85	1.01	1.02		0.1467	0.090916494
Sitia	PQ	0.85	4.8327		1.0481888	0.163	0.101018327
Agios Nikolaos	PQ	0.85	0.6516		0.1413288	0.4564	0.282851316
Ierapetra	PQ	0.85	0		0	0.20375	0.126272909
Stalida	PQ	0.85	0		0	0.6357	0.393971476
Praitorion	PQ	0.85	0		0	0.13855	0.085865578
Moires	PQ	0.85	0.9774		0.2119932	0.38305	0.237393069
Agias Barbaras	PQ	0.85	0.8145		-0.176661	0.12225	0.075763745
Ammou	PQ	0.85	0		0	0.7498	0.464684305
Spili	PQ	0.85	0		0	0.1956	0.121221993
Rethumno	PQ	0.85	0.543		-0.117774	0.6846	0.424276974
Vrisses	PQ	0.85	0		0	0.2282	0.141425658
Aguias	PQ	0.85	0		0	0.1304	0.080814662
Kissamos	Swing	0.85	1.0317	1.02	0.2237706	0.163	0.101018327

The face validity of the scenarios was also confirmed by ensuring that the system's behavior in these conditions aligned with expectations from both theoretical knowledge and real-world experience. For instance, voltage violations outside the acceptable range and overloading of transmission lines would typically signal potential issues in system stability or capacity [18]. The results of the analysis demonstrated that all simulated conditions remained within the expected operational limits, supporting the face validity of the model. These steps confirm that the research provides plausible and reasonable results that would be recognized as valid by professionals in the field.

3.3. CONTENT RELIABILITY AND VALIDITY

The reliability and validity of the results in the power flow analysis using the Newton-Raphson method are ensured through the precise application of the method within the InterPSS software, alongside adherence to established industry standards. The Newton-Raphson method, widely used for solving nonlinear equations in power systems, provides reliable results as it allows for rapid convergence and high accuracy in power flow analysis [19]. The voltages at the system buses must lie within the range of 1.05 P.U. < V < 0.95 P.U., as required for proper system operation [20]. Furthermore, the 202 MVA, 124 MVA, and 170 MVA transfer limits for the 150 kV lines provide a safe basis for avoiding overloads and effectively distributing power throughout the network [14]. The use of InterPSS ensures that the simulation results are both valid and reliable, confirming that the network operates within technical and operational limits.

4. RESULTS

4.1. FIRST SCENARIO

The load flow analysis using the Netwon-Raphson method, with a maximum of 50 iterations and a convergence threshold of 0.0001 [19]. We examine the voltage (P.U.), levels of all buses. The voltage fluctuation range is normally between 0.95 P.U. < V < 1.05 P.U. [20]. As observed, no bus voltage exceeds these limits. Therefore, no operational issues are present in this scenario (1-Chania: 1.02 P.U., 2-Heraklion: 1.02 P.U., 3-Atherinolakkou: 1.02 P.U., 4-Sitia: 1.0153 P.U., 5-Agios Nikolaos: 0.9902 P.U., 6-Ierapetra: 0.9981 P.U., 7-Stalida: 0.9903 P.U., 8-Praitorion: 0.9953 P.U., 9-Moires: 0.996 P.U., 10-Agias Barbaras: 1.0043 P.U., 11-Ammou: 0.9984 P.U., 12-Spili: 0.9926 P.U., 13-Rethumno: 0.9949 P.U., 14-Vrisses: 1.0169 P.U., 15-Aguias: 1.0188 P.U., 16-Kissamos: 1.02 P.U.). There was no issue in this scenario, as all bus voltages remained within the permissible limits (Figure 3).

Next, the transmitted power in each branch of the system was examined. If the power limits were exceeded (overloading), additional branches would be required to redistribute the power flow. The transmission power limits used for the 150 kV transmission lines are as follows MVARating1= 202 MVA, MVARating2= 124 MVA MVARating1= 170 [14]. The analysis focused on the highest transmission power limit, 202 MVA. The results, which $S=\sqrt{P^2+Q^2}$ show the apparent power (S) for each branch, while P and Q represent the active and reactive power, respectively indicate that there was not a power flow over flow overload in several branches [14].

4.2. SECOND SCENARIO

The second scenario is simulated in the same manner as scenario 1, with the only difference being that wind power generation is multiplied by a factor of 5.4, resulting in a total of 1000MW = 10 P.U. The load flow analysis using the Newton-Raphson method, with a maximum of 50 iterations and a convergence threshold of 0.0001 [19].

We examine the voltage (P.U.), levels of all buses. The voltage fluctuation range is normally between 0.95 P.U. < V < 1.05 P.U. [20]. As observed, no bus voltage exceeds these limits. Therefore, no operational issues are present in this scenario (1-Chania: 1.02 P.U., 2-Heraklion: 1.02 P.U., 3-Atherinolakkou: 1.02 P.U., 4-Sitia: 1.0079 P.U., 5-Agios Nikolaos: 0.9552 P.U., 6-Ierapetra: 0.9612 P.U., 7-Stalida: 0.9656 P.U., 8-Praitorion: 0.9626 P.U., 9-Moires: 0.9706 P.U., 10-Agias Barbaras: 0.9903 P.U., 11-Ammou: 0.982 P.U., 12-Spili: 0.9556 P.U., 13-Rethumno: 0.9579 P.U., 14-Vrisses: 0.9961 P.U., 15-Aguias: 1.0131 P.U., 16-Kissamos: 1.02 P.U.). There was no issue in this scenario, as all bus voltages remained within the permissible limits (Figure 4).

Next, the transmitted power in each branch of the system was examined. If the power limits were exceeded (overloading), additional branches would be required to redistribute the power flow. The transmission power limits used for the 150 kV transmission lines are as follows MVARating1= 202 MVA, MVARating2= 124 MVA MVARating1= 170 [14]. The analysis focused on the highest transmission power limit, 202 MVA. The results include the apparent power (S) for each branch, calculated as , and presented in the last column. Futhermore, P and Q represent the active and reactive power, respectively, indicating that there was no power flow overload in several branches [14].

Table 3 presents the branches where current flow overloads occurred. To redistribute the power, additional branches will be required. These branches are located between the following buses: 1-13, 1-15, 1-14, 1-16, 2-14, 3-6, 6-4, 13-1, 14-1, 14-2, 15-1, 15-16, 16-1, 16-15. The corresponding power flows are presented in Table 3.

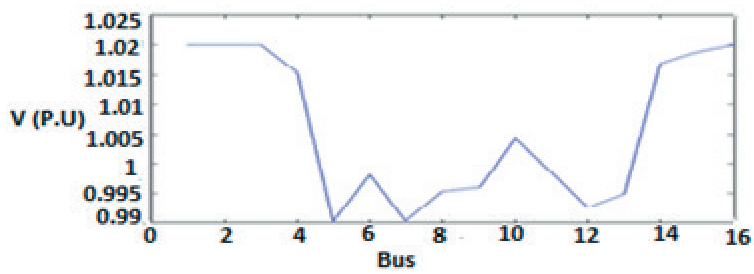

Figure 3. Voltage diagram

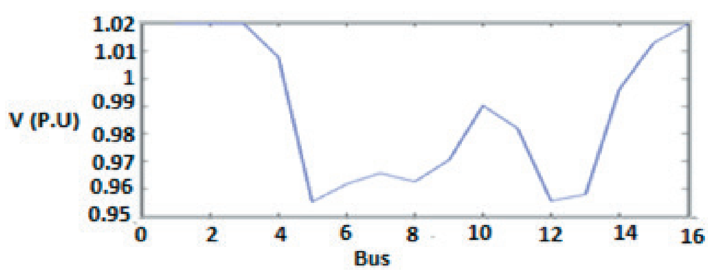

Figure 4. Voltage diagram

Table 3. Power Flows in the Branches

Previous Bus	Net Bus	P (MW)s	Q (MVAr)	$S=\sqrt{P^2+Q^2}$ (MVA)
1	13	-280.8	178.81	332.8988677
	15	261.29	-31.22	263.148537
	14	-206.14	111.36	234.2962851
	16	347.64	-44.11	350.4272559
2	14	254.74	-2.06	254.7483291
3	6	256.91	48.08	261.3703015
	6	291.81	-34.33	293.8224379
6	4	-265.65	84.86	278.8747785
	3	-246.91	-11.38	247.1721111
	1	304.23	-86.73	316.3510484
14	1	211.67	-92.07	230.8269347
	2	-233.67	78.07	246.3667871
15	1	-252.67	62.6	260.3092179
	16	239.67	-70.6	249.852094
16	1	-330.32	112.37	348.910188
	15	-235.48	85.59	250.5523468

Table 4. Power Flows in the Branches after System Reinforcement

Previous Bus	Net Bus	P (MW)s	Q (MVAr)	$S=\sqrt{P^2+Q^2}$ (MVA)	MVARating1
1	13	-266.2	140.09	300.8116489	404
	15	279.3	-51.61	284.0283121	404
	14	-263.19	97.5	280.6692468	404
	16	372.08	-69.32	378.4822173	404
2	14	304.22	-41.74	307.0700832	404
	11	-104.15	107.94	149.9942202	202
	7	-127.68	104.94	165.2712498	202
	10	-65.18	84.57	106.773205	202
	13	142.79	2.96	142.8206767	202
3	6	220.97	51.26	226.8376699	404
	4	-133.97	52.14	143.7586189	202
4	3	135.27	-49.5	144.0424344	202
	6	328.73	-64.5	334.9980043	404
5	6	-179.05	-1.81	179.0591483	202
	7	199.05	-40.19	203.0668328	202
6	4	-312.07	82.92	322.8984535	404
	3	-217.21	-48.37	222.5305395	404
	11	188.08	-32.21	190.8181608	202

Previous Bus	Net Bus	P (MW)s	Q (MVAr)	$S = \sqrt{P^2 + Q^2}$ (MVA)	MVARating1
	5	180.8	7.15	180.9413234	202
	8	140.4	-21.5	142.0366502	202
7	5	-194.4	55.77	202.2415707	202
	2	131.4	-94.77	162.0102247	202
8	6	-135.96	31.4	139.5388175	202
	9	122.96	-39.4	129.1182466	202
9	8	-121.4	42.23	128.5353372	202
	10	-1.62	-62.05	62.07114386	202
	12	182.02	-24.18	183.6190426	202
10	9	1.99	60.53	60.56270304	202
	2	67.01	-84.53	107.8687211	202
11	6	-180.06	57.56	189.0363912	202
	2	106.06	-103.56	148.2342646	202
12	9	-177.54	37.98	181.5569663	202
	13	158.54	-49.98	166.2315614	202
13	2	-138.19	6.46	138.3409112	202
	12	-155.71	57.97	166.1509103	202
	1	275.9	-117.43	299.8509878	404
14	1	267.16	-90.15	281.9600825	404
	2	-289.16	76.15	299.0189427	404
15	1	-274.38	61.25	281.1333258	404
	16	261.38	-69.25	270.3979787	404
16	1	-362.1	99.22	375.4477572	404
	15	-258.99	73.54	269.2284378	404

In addition, power flow overloads were observed in the branches, resulting in the network being unable to operate under these conditions. Particularly in the branches between the buses 1-13 (332.9 MVA), 16-1(350.4 MVA), 1-15(263.1 MVA), 1-14(234.3 MVA), 16-15(250.6 MVA), 2-14(254.7 MVA), 6-4(293.8 MVA), and 6-3(261.7 MVA), there was an overload exceeding MVARating1, and a second identical circuit was added. This was achieved by halving the resistance values R (P.U.) and the inductive reactance values X (P.U.), and by doubling the transverse conductance 1/2B (P.U.) and the power transfer limits MVARating1, MVARating2, MVARating3 [14]. The results of the network after these changes to enhance the system are presented in Table 4.

Table 4 presents the power flows in each branch of the system after the reinforcement measures were implemented. These measures were carried out by adding additional circuits and adjusting the system parameters, such as halving the resistance and reactance values and doubling the power transfer limits, as described earlier. The table shows the updated active and reactive power flows in each branch following these changes to relieve overloading and improve system stability. After the necessary changes were made, it was observed that the branches are now within the permissible limits and are no longer overloaded. As a result, the system is functioning without any issues.

5. DISCUSSION

The results obtained from the InterPSS simulations confirm its effectiveness in analyzing power system performance. In the first scenario, where load values were maintained near their current levels with 100% of the existing wild power generation, voltage levels remained within permissible limits, and no power flow overloads were observed. This indicates that under these conditions, the system can operate reliably without modifications. In comparison, Kumar et al. [21] demonstrated that InterPSS provides results comparable to other software for flow analysis while offering a more user-friendly interface. Similarly, Zhou and Huang [11] highlighted the software's efficiency in real-time simulations, making it strong software.

In the second scenario, where wind power generation was increased to 1000 MW while keeping load levels constant, significant power overloads were detected in multiple network branches. Although voltage levels remained within acceptable limits, the increased wind penetration caused congestion in several transmission lines, rendering the system unable to function under these conditions. The findings align with Brahmendra Kumar et al. [22], who emphasized the necessity of grid reinforcements when integrating large-scale renewable energy sources. Their study confirmed that high wind power energy generation can lead to transmission congestion, a result also observed in the present study. Additionally, Medina et al. [23] examined transmission congestion in renewable-dominated grids and recommended expanding transmission capacity as an effective solution, further validating the approach proposed in this study.

Finally, the proposed solution involved adding new transmission lines between overloaded buses, thereby redistributing power flow and mitigating the overloading issue, ultimately allowing stable system operation which is in line with the findings of Wang and Li [24].

6. CONCLUSIONS

The research demonstrated that while InterPSS is a robust tool for power system analysis, grid stability under high renewable energy penetration remains a critical challenge. The results emphasize that without proper infrastructure reinforcement, increased wind power integration can lead to significant operational constraints. This highlights the urgent need for strategic transmission expansions to ensure a resilient and reliable power grid.

7. ACKNOWLEDGMENT

The authors would like to acknowledge the support at the Technical University of Crete, which facilitated this research. Appreciation is extended to colleagues and peers for their valuable discussions and insights throughout the study. Additionally, gratitude is expressed to the developers of InterPSS for making an open-source platform available for comprehensive power system analysis.

REFERENCES

[1] P. Tsvetkov, P. Samuseva, L. Nikolaychuk, "The research of the impact of energy efficiency on mitigating greenhouse gas emissions at the national level," *Energy Conversion and Management,* vol. 314, p. 118671, 2024, https://doi.org/10.1016/j.enconman.2024.118671.

[2] K. Devadasa, N, H. Laxminarayana, "The role of renewable energy in mitigating climate change," *Journal of Visual and Performing Arts*, 2024, https://doi.org/10.29121/shodhkosh.v4.i1.2023.2786.

[3] F. S. Chien, K. Y. Chau, M. Sadiq, G. L. Diep, T. K. Tran, T. H. A. Pham, "What role renewable energy consumption, renewable electricity, energy use and import play in environmental quality?," *Energy report,* vol. 10, pp. 3826-3834, Nov. 2023, https://doi.org/10.1016/j.egyr.2023.10.024

[4] A. Ramos, "Sustainabilty assessment in waste management: An explotary study of the social perspective in waste-to-energy cases," *Journal of Cleaner Production*, vol. 475, 2024, https://doi.org/10.1016/j.jclepro.2024.143693.

[5] M. Busu, C. L. Trica, "Sustainability of Circular Economy Indicators and Their Impact on Economic Growth of the European Union," *Sustainability*, vol. 11, no. 19, p. 5481, 2019, https://doi.org/10.3390/su11195481.

[6] J. Rosak-Szyrocka, A. A. S. Allahham, J. Zywiotek, J. A. Turi, A. Das, "Expectations for renewable energy, and its impacts on quality of life in European union countries," *Management Systems In Production Engineering*, vol. 3, no.2, pp. 128-137, 2023, https://doi.org/10.2478/mspe-2023-0015.

[7] F. Wang, J. D. Harindintwali, K. Wei, et al., "Climate change: Strategies for mitigation and adaptation," T*he Innovation Geoscience,* vol. 1, no. 1, p. 100015, 2023, https://doi.org/10.59717/j.xinn-geo.2023.100015.

[8] L. Chen, G. Msigwa, M. Yang, A. Osman, S. Fawzy, D. W. Rooney, P-S. Yap, "Strategies to achieve a carbon neutral society: a review," *Environ Chem Lett,* vol. 20, pp. 2277-2310, 2022, https://doi.org/10.1007/s10311-022-01435-8.

[9] T. Z. Ang, M. Salem, M. Kamarol, H. S. Das, M. A. Nazari, N. Prabaharan, "A comprehensive study of renewable energy sources: Classifications, challenges and suggestions," *Energy Strategy Reviews*, vol. 43, 2022, https://doi.org/10.1016/j.esr.2022.100939.

[10] M. A. V. Rad, A. Kasaeian, X. Niu, K. Zang, O. Mahian, "Excess electricity problem in off-grid hybrid renewable energy systems: Acomprehensive review from challenges to prevalent solutions. *Renewable Energy*, vol. 212, pp. 538-560, 2023, https://doi.org/10.1016/j.renene.2023.05.073.

[11] M. Zhou, Q. Huang, "InterPSS A New Generation Power System Simulation Engine," *Engineering, Computer Science,* 2017, https://doi.org/10.48550/arXiv.1711.10875

[12] InterPSS Development Team, "InterPSS Community," [Online]. Available: https://sites.google.com/a/interpss. org/interpss/Home. [Accessed: Mar. 18, 2025].

[13] E. Loukarakis, "Isolated Electrical Power Systems Optimal Interconnections Planning," Diploma Thesis, Technical University of Crete, Chania, 2012.

[14] P. Kundur, "Power System Stability and Control," McGraw-Hill, 1994.

[15] J. D. Glover, M. S. Sarma, T. J. Overbye, "Power System Analysis and Design," 5th ed., Cengage Learning, 2011.

[16] A. J. Wood, B. F. Wollenberg, "Power Generation, Operation, and Control," 2nd ed., Wiley, 2012.

[17] R. Billinton, R. N. Allan, "Reliability Evaluation of Power Systems," Springer, 1996.

[18] H. Saadat, "Power System Analysis," 3rd ed. McGraw-Hill, 2010.

[19] A. Ahmadi, M. C. Smith, E. R. Collins, V. Dargahi, S. Jin, "Fast Newton-Raphson Power Flow Analysis Based on Sparse Techniques and Parallel Processing," in *IEEE Transactions on Power Systems*, vol. 37, no. 3, pp. 1695-1705, 2022, https://doi.org/10.1109/TPWRS.2021.3116182

[20] K. Chaiyaphun, P. Santiprapan, K. Areerak, "A Modified Variable Power Angle Control for Unified Power Quality Conditioner in a Distorted Utility Source," *Energies*, vol. 17, no. 12, p. 2830, 2024, https://doi.org/10.3390/en17122830.

[21] Y. Kumar, V. K. Devabhaktuni, S. Vemuru, "Comparison of power system simulation tools with load flow study cases," *Institute of Electrical and electronics Engineers*, 2015, https://doi.org/10.1109/EIT.2015.7293355.

[22] G. V. Brahmendra Kumar, K. Ratnam, P. Kaliannan, S. Padmanaban, J. B. Holm-Nielsen, "Large Scale Renewable Energy Integration: Issues and Solutions, *Energies*," vol. 12, no. 10, 2019, https://doi.org/10.3390/el12101996

[23] C. Medina, G. G. Gonzales, "Transmission Grids to Foster High Penetration of Large-Scale Variable Renewable Energy Sources - A Review of Challenges, Problems, and Solutions," *International Journal of Renewable Energy Technology*, vol. 12, no. 1, pp. 146-169, Jan. 2022, https://doi.org/10.20508/ijrer.v12i1.12738.g8400.

[24] H. Wang, Z. Li, "A Review of Power System Transient Stability Analysis and Assessment," Prognostics and System Health Management Conference (PHM-Qingdao), China, 2019, https://doi.org/10.1109/PHM-Qingdao46334.2019.8942834.